



Published in final edited form as:

J Neurosurg. 2009 October ; 111(4): 701. doi:10.3171/2009.3.JNS0990.

Wireless Instantaneous Neurotransmitter Concentration System—based amperometric detection of dopamine, adenosine, and glutamate for intraoperative neurochemical monitoring

Filippo Agnesi, M.S.¹, Susannah J. Tye, Ph.D.², Jonathan M. Bledsoe, M.D.², Christoph J. Griessenauer, M.D.², Christopher J. Kimble, M.A.³, Gary C. Sieck, Ph.D.¹, Kevin E. Bennet, B.S.Ch.E., M.B.A.³, Paul A. Garris, Ph.D.⁴, Charles D. Blaha, Ph.D.⁵, and Kendall H. Lee, M.D., Ph.D.^{1,2}

¹Department of Physiology and Biomedical Engineering, Mayo Clinic, Rochester, Minnesota

²Department of Neurologic Surgery, Mayo Clinic, Rochester, Minnesota

³Department of Division of Engineering, Mayo Clinic, Rochester, Minnesota

⁴Department of Biological Sciences, Illinois State University, Normal, Illinois

⁵Department of Psychology, University of Memphis, Tennessee

Abstract

Object—In a companion study, the authors describe the development of a new instrument named the Wireless Instantaneous Neurotransmitter Concentration System (WINCS), which couples digital telemetry with fast-scan cyclic voltammetry (FSCV) to measure extracellular concentrations of dopamine. In the present study, the authors describe the extended capability of the WINCS to use fixed potential amperometry (FPA) to measure extracellular concentrations of dopamine, as well as glutamate and adenosine. Compared with other electrochemical techniques such as FSCV or high-speed chronoamperometry, FPA offers superior temporal resolution and, in combination with enzyme-linked biosensors, the potential to monitor nonelectroactive analytes in real time.

Methods—The WINCS design incorporated a transimpedance amplifier with associated analog circuitry for FPA; a microprocessor; a Bluetooth transceiver; and a single, battery-powered, multilayer, printed circuit board. The WINCS was tested with 3 distinct recording electrodes: 1) a carbon-fiber microelectrode (CFM) to measure dopamine; 2) a glutamate oxidase enzyme-linked electrode to measure glutamate; and 3) a multiple enzyme-linked electrode (adenosine deaminase, nucleoside phosphorylase, and xanthine oxidase) to measure adenosine. Proof-of-principle analyses included noise assessments and in vitro and in vivo measurements that were compared with similar analyses by using a commercial hardwired electrochemical system (EA161 Picostat, eDAQ; Pty Ltd). In urethane-anesthetized rats, dopamine release was monitored in the striatum following deep brain stimulation (DBS) of ascending dopaminergic fibers in the medial forebrain bundle (MFB). In separate rat experiments, DBS-evoked adenosine release was monitored in the ventrolateral thalamus. To test the WINCS in an operating room setting resembling human neurosurgery, cortical

Address correspondence to: Kendall H. Lee, M.D., Ph.D., Department of Neurologic Surgery, Mayo Clinic, 200 First Street Southwest, Rochester, Minnesota 55905. lee.kendall@mayo.edu.

Portions of this work were presented in poster form at the National Institutes of Health Neural Interfaces Conference in Cleveland, Ohio, in July 2008, and at the Society for Neuroscience meeting in Washington, DC, in November 2008. Portions of this work were also presented in abstract form at the American Society for Stereotactic and Functional Neurosurgery Biennial Meeting in Vancouver, BC, Canada, in June 2008, and at the American Academy of Neurological Surgery Annual Meeting in Sedona, Arizona, in September 2008.

glutamate release in response to motor cortex stimulation (MCS) was monitored using a large-mammal animal model, the pig.

Results—The WINCS, which is designed in compliance with FDA-recognized consensus standards for medical electrical device safety, successfully measured dopamine, glutamate, and adenosine, both in vitro and in vivo. The WINCS detected striatal dopamine release at the implanted CFM during DBS of the MFB. The DBS-evoked adenosine release in the rat thalamus and MCS-evoked glutamate release in the pig cortex were also successfully measured. Overall, in vitro and in vivo testing demonstrated signals comparable to a commercial hardwired electrochemical system for FPA.

Conclusions—By incorporating FPA, the chemical repertoire of WINCS-measurable neurotransmitters is expanded to include glutamate and other nonelectroactive species for which the evolving field of enzyme-linked biosensors exists. Because many neurotransmitters are not electrochemically active, FPA in combination with enzyme-linked microelectrodes represents a powerful intraoperative tool for rapid and selective neurochemical sampling in important anatomical targets during functional neurosurgery.

Keywords

deep brain stimulation; motor cortex stimulation; pig; amperometry; dopamine; glutamate; adenosine; rat

Deep brain stimulation and MCS have been successful in treating a variety of neuropsychiatric disorders.^{22,29,45} Furthermore, there is now a growing body of evidence indicating that one important mechanism of action of DBS and MCS is the modulation of neural networks through neurotransmitter release.^{29,44} However, the role of specific neurotransmitters in this phenomenon and the kinetics of release are only now beginning to be elucidated. Thus, the development of tools to measure neurotransmitter release in humans may be important in elucidating the mechanism of action as well as improving the neuromodulation technology. In a companion paper,⁸ we have described the development of a small, battery-powered, wireless device called the WINCS, which supports the electrochemical recording technique of FSCV to measure dopamine extracellular concentrations in the brain. When combined with a CFM, FSCV is the technique of choice for measurements of electroactive analytes, such as dopamine, in anesthetized or freely moving animals. The background-subtracted cyclic voltammogram serves as a chemical signature to identify the neurochemical of interest.¹⁸ However, FSCV is prone to changes in background current and to temporal distortion by analyte adsorption to the CFM.³

An alternative to FSCV is the electrochemical technique FPA. During FPA, a fixed potential is applied to the probe at a level sufficient to oxidize the analyte of interest. Compared with other real-time electrochemical techniques, such as FSCV or high-speed chronoamperometry, FPA offers superior temporal resolution, with the capability of measuring analyte flux to the probe as fast as the data acquisition permits.^{6,18,42} An additional advantage of FPA is that it can be coupled to an enzyme-linked biosensor, thus enabling monitoring of nonelectroactive neurochemicals such as glutamate, which has been implicated as being released during electrical stimulation of the brain, such as DBS and MCS.^{21,32} A common configuration for a glutamate biosensor is the coating of the enzyme glutamate oxidase onto a platinum microwire. Glutamate reaction with this enzyme generates hydrogen peroxide, which is then oxidized at the platinum surface of the probe by using FPA.

Similarly, the purine metabolite adenosine, which has recently been implicated in the tremor-suppressant action of DBS of the thalamus,⁴ can also be measured with FPA by using an enzyme-linked biosensor. Although this electroactive neurochemical can be measured with FSCV by using CFMs, it oxidizes at a much higher potential (+1.3 V) than dopamine (+0.6

V).^{13,25} The enzyme-linked biosensor consists of a 3-enzyme coating (adenosine deaminase, nucleoside phosphorylase, and xanthine oxidase³³) that is used to react with adenosine to generate inosine (by removal of an amino group), further converted to hypoxanthine (by removal of the ribose ring), and then oxidized to uric acid with the production of hydrogen peroxide.

In this paper, the further development of the WINCS is described, expanding on the FSCV capabilities established in our companion article⁸ to include FPA used in combination with CFMs to measure dopamine, or with enzyme-linked biosensors to measure adenosine and glutamate. Recordings of glutamate levels made using WINCS-based FPA were also successfully obtained in a large-animal model mimicking human functional neurosurgical procedures. These results demonstrate that the WINCS represents a powerful device that may be used during neurosurgery to monitor various neurochemicals implicated in a number of neurological and psychiatric disorders. Therefore, this device may prove useful for precision placement of stimulating electrodes during functional neurosurgery and in elucidating the mechanism of action of neurosurgical therapies such as DBS and MCS.

Methods

The WINCS Hardware Configuration

In our companion article,⁸ we described the development of the WINCS hardware that combines FSCV with digital telemetry to perform microsecond electrochemical measurements at a CFM implanted in the brain. Briefly, the WINCS device (Fig. 1 *upper*) incorporates a transimpedance amplifier and associated analog circuitry for electrochemistry; a microprocessor with a dual analog-to-digital converter and digital-to-analog ports; and a Bluetooth transceiver (all on a single, rechargeable lithium-polymer battery-powered, multilayer, printed circuit board). The device can be packaged in a sterilizable polycarbonate case (Fig. 1 *lower*).

The WINCS in the FPA mode uses one of the microprocessor's digital-to-analog converters to apply a fixed potential to a CFM or enzyme-linked biosensor. Sensor current is converted to a voltage at 1 kHz by the transimpedance amplifier, converted to a digital data stream by one of the microprocessor's analog-to-digital converters, and then wirelessly transmitted to the WINCS support station. The support station consists of a Windows-XP laptop running custom software that remotely (wirelessly) controls the parameters and operation of WINCS, such as starting and stopping data acquisition and transmission, modifying the applied fixed potential, and changing the sampling rate. The FPA data are saved to disk as a sequence of unsigned 2-byte integers, a format suitable for postprocessing by various software applications, such as MATLAB (The MathWorks, Inc.) or LabVIEW (National Instruments).

Fixed Potential Amperometry

The FPA recordings performed in a 2-electrode configuration with the WINCS were compared with those obtained using a commercially available hardwired electrochemical recording system (eDAQ, Pty Ltd.) that consisted of a potentiostat (EA161 Picostat) in conjunction with an analog-to-digital signal converter-recorder (e-corder) run by Chart software. The FPA study performed with a CFM was used to test the WINCS reliability by measuring dopamine *in vitro* or electrically evoked dopamine release *in vivo*. During these experiments, the applied potential was held at +0.8 V versus an Ag/AgCl reference/counter electrode.

Commercially available biosensors that are sensitive to adenosine (Sarissa Biomedical) and glutamate (Pinnacle Technology, Inc.) were used to test the capability of the WINCS to measure these molecules. These sensors consisted of a platinum wire coated with one or more enzymes

and a selectively permeable membrane to block compounds that have the potential for electroactive interference. Glutamate is converted by the enzyme glutamate oxidase to α -ketoglutarate, generating hydrogen peroxide that is subsequently oxidized at the platinum surface, producing an amperometric signal whose magnitude is directly proportional to the concentration of the analyte. Adenosine deaminase converts adenosine to inosine by removal of an amino group. Inosine is subsequently converted to hypoxanthine by the enzyme nucleoside phosphorylase with the removal of the ribose ring. Xanthine oxidase subsequently oxidizes hypoxanthine to xanthine, and further to uric acid, with the production of hydrogen peroxide. The hydrogen peroxide at the adenosine sensor is oxidized in a similar manner as at the glutamate sensor, producing an amperometric signal. For both in vitro and electrically evoked release in vivo, the applied potential was set to values indicated by the manufacturers of each sensor (+0.5 and +0.6 V for adenosine and glutamate, respectively).

In Vitro Testing of the WINCS-Based FPA

Analysis of Electromagnetic Interference—To evaluate the susceptibility of WINCS-based FPA recordings to electromagnetic interference, measurements were collected by the WINCS and compared with those obtained simultaneously with the eDAQ system in a hospital neurosurgical operating room. A dummy cell consisting of a standard $100 \pm 1\%$ M Ω resistor was connected to each system, and they were placed on the operating room table within 30 cm of each other. A fixed potential of +0.8 V was applied to the dummy cell, and various electrical devices normally used during functional neurosurgery were turned on and off sequentially to evaluate noise perturbations. Oxidation current dynamics recorded in vivo by FPA are slow enough to permit 10-Hz low-pass filtering to reduce noise, while preserving the signal of interest.^{16,30,42,43} Thus, to mimic the filter settings typically used for in vivo testing (described later), the FPA signals recorded from the dummy cell with the WINCS and the eDAQ system were also filtered at 10 Hz.

Calibration of CFMs and Enzyme-Linked Biosensors—Prior to their use in vivo, flow injection analysis was used with both the WINCS and the commercial eDAQ system for in vitro FPA calibration of CFMs for dopamine. In this well-established procedure for device testing and sensor calibration,²⁸ a CFM was positioned in the center of a Plexiglas reservoir (flow cell) in which a flowing stream of physiological buffer at room temperature (0.01 M PBS, pH 7.6) was pumped at a constant rate of 4 ml/minute.⁸ An electronic valve allowed a 1-ml volume loop containing 2.5, 5, or 10 μ M of dopamine hydrochloride (Sigma-Aldrich, Inc.) to be injected into the flowing stream of buffer for 5 seconds. An Ag/AgCl reference/counter electrode positioned on the periphery of the reservoir in contact with the buffer solution completed the 2-electrode system.

Using the commercially available enzyme-linked biosensors for glutamate and adenosine, in vitro WINCS-based FPA measurements of various concentrations of these substances were performed at room temperature prior to their use in vivo. Using similar calibration protocols specified by the respective manufacturers of these sensors, 5 ml of a 50- μ M adenosine solution (Sigma-Aldrich, Inc.) was added to a beaker containing 20 ml of PBS to provide a single 10- μ M step in adenosine concentration. Glutamate sensitivity was assessed by adding 250 μ l of a 5-mM L-glutamate solution (Sigma-Aldrich, Inc.) to a 25-ml volume of PBS stirred with a magnetic stirrer for three 50- μ M steps in glutamate concentration.

In Vivo Testing of the WINCS-Based FPA

Experimental Animals—For proof-of-principle evaluation of the functionality of the WINCS-based FPA recordings in vivo, 5 adult male Sprague-Dawley rats weighing between 300 and 400 g were used to record electrically stimulated release of dopamine (4 rats) and adenosine (1 rat). One female pig weighing 25 kg was used for in vivo glutamate recordings.

The animals were housed under standard conditions with free access to food and water. Care was provided in accordance with National Institutes of Health guidelines (Publication 86–23) and approved by the Mayo Clinic Institutional Animal Care and Use Committee.

Dopamine Recordings—Four of the rats were anesthetized with 1.5 g/kg intraperitoneally injected urethane (Sigma-Aldrich, Inc.) and then mounted onto a commercially available stereotactic frame (David Kopf, Inc.). Multiple bur holes were drilled for implantation of the reference/counter and stimulating electrodes and the CFM. Stereotactic coordinates were obtained from the Paxinos and Watson rat atlas by using a flat skull orientation and the bone suture landmark bregma as the reference point. A bipolar stimulating electrode (MS 303/2; Plastics One) with the tips separated by 1 mm was placed within the MFB containing dopaminergic axons at the following coordinates: AP -4.6 , ML $+1.2$, and DV -8.0 mm from dura mater. The CFM was positioned in the dorsomedial striatum at the following coordinates: AP $+1.2$, ML $+2.0$, and DV -4.6 to -6.0 mm from dura mater, and it was adjusted to obtain a robust stimulation-evoked FPA signal. The reference/counter electrode was inserted into superficial cortical tissue contralateral to the CFM and stimulating electrode. Electrical stimulation of the MFB consisted of a train of 60-Hz monophasic pulses ($900 \mu\text{A}$, 2-msec pulse width) applied for 1, 2, or 4 seconds via an optical isolator and programmable pulse generator (Iso-Flex/Master-8, AMPI). Stimulation of the MFB was applied 3 times with an interval between stimulations equal to 5 seconds per every pulse delivered, and the responses were averaged.

In some animals, the same surgical procedure and stimulation parameters were used to compare the WINCS-based FPA and the FSCV recordings of MFB stimulation-evoked dopamine release. As in our companion study showing the utility of WINCS-based FSCV,⁸ this recording procedure differs from FPA in that the potential between the CFM and reference/counter electrode is cycled 10 times per second by using a triangle wave between -0.4 and $+1$ V, and then back to -0.4 V, at a speed of 300 V/second. The current recorded during a potential sweep yields a combination of capacitive and faradic (oxidation/reduction) current. A sufficient number of potential sweeps are averaged before stimulation to yield a baseline template that is then subtracted from every subsequent sweep to obtain faradic currents corresponding to the unique electrochemical signal of dopamine oxidation and reduction (see Fig. 4D *inset*). Thus, the heights of the peaks in background-subtracted voltammograms are directly proportional to the concentration of dopamine that is oxidized and reduced at the CFM surface. The peak heights of dopamine oxidation, in turn, are displayed with respect to time and, together with the peak heights of dopamine reduction, graphed in a pseudocolor plot (see Fig. 4D, *upper* and *lower* panel, respectively). These measures provide enhanced selectivity of FSCV compared with FPA, for recording real-time, chemically resolved changes in dopamine at CFMs in freely moving animals.¹⁸

Adenosine Recordings—A similar procedure to that described above was used to prepare the rat used for in vivo testing of the WINCS with the adenosine biosensor. Electrical stimulation was delivered through a scaled-down version of a typical DBS electrode composed of 4 ring contacts along the electrode shaft (0.28-in diameter; 4 contacts, 0.02-in size; with 0.02-in spacing between contacts). The tips of the stimulating electrodes and sensor probes were mounted within 0.5 mm of each other on a single stereotactic electrode carrier, with the biosensor's tip midway between contacts 1 and 2 of the stimulating electrode. The stimulating electrode was implanted on the border of the VL thalamus at the following coordinates: AP -2.4 , ML $+2.2$, and DV -6.0 mm from dura mater, and the adenosine sensor was placed more medially, and thus within the VL thalamus. The reference/counter electrode was placed in superficial contact with cortical tissue contralateral to the stimulating and recording electrodes. After achieving a stable baseline signal, monophasic 0.1-msec constant current pulses were applied for 10-second durations across the DBS electrode contacts 0 (negative) and 3 (positive)

at various current intensities (0.5–2 mA) and fixed frequency (100 Hz), and at various frequencies (50–200 Hz) and fixed intensity (1 mA). Calibration before implantation of the adenosine biosensor with the protocol described above was used to convert oxidation current recorded in vivo into adenosine concentrations.

Glutamate Recordings—Under the care of a certified veterinarian technician, the pig was sedated with a combination of 5–6 mg/kg telazole and 2 mg/kg xylazine administered intraperitoneally prior to intubation. Continuous anesthesia was maintained with 1% isoflurane (all 3 drugs supplied by the Mayo Clinic Pharmacy) for the rest of the procedure. The pig was then placed in an in-house built, MR imaging-compatible stereotactic frame,⁷ followed by exposure of part of the left motor cortex via a midline scalp incision and craniotomy. A Medtronic 3389 DBS lead mounted onto a stereotactic electrode holder was used as the stimulating electrode. The glutamate sensor was secured to the same holder within 0.5 mm of the stimulating electrode and with its sensing cavity positioned between contacts 1 and 2. The 2 were then lowered vertically until all of the stimulating electrode's contacts were inserted into the cortex. After achieving a stable baseline signal, monophasic 100- μ sec constant current pulses were applied for 10 seconds at various current intensities (0.5–2 mA, 100 Hz, contact 0 positive and 3 negative). Calibration before implantation of the glutamate biosensor with the protocol described above was used to convert oxidation current recorded in vivo to glutamate concentrations.

Results

In Vitro Testing of the WINCS-Based FPA

Analysis of Electromagnetic Interference—As expected, an average current of ~ 8 nA was recorded with both the WINCS and the eDAQ system, with an applied fixed potential of +0.8 V across a 100-M Ω resistor (Fig. 2). The magnitude of the noise envelope recorded with the WINCS appeared more marked than with the eDAQ system, with an SD of ± 8.3 and ± 2.1 pA, respectively, measured in the first 20 seconds of unperturbed recording. Electrical interference created by activation of the electrocauterizer (monopolar and bipolar settings) or the pneumatic drill evoked detectable disturbances in the baseline signal recorded with the eDAQ system that were difficult to detect in the higher average noise envelope recorded by the WINCS. Turning the overhead surgical lights on and off had no significant impact on the baseline FPA signals recorded by either system. However, noise elicited by waving a hand over the dummy cell generated a significantly greater disturbance in the baseline signal recorded by the eDAQ system compared with the WINCS. The WINCS has a resolution of 16 bits, and a dynamic range > 1.2 mA is needed to perform FSCV. As a consequence, the smallest current increment theoretically measurable in the absence of noise is ~ 19 pA. As a function of the SD of the recorded baseline signal in this test, the effective resolution of the WINCS analog-to-digital converter was ~ 14 bits, allowing current measurements on the order of a few hundred picoamperes. Although higher resolution is always a desirable feature, the intrinsic noise levels of the WINCS-based FPA recordings were found to be acceptable to measure oxidation currents both in vitro and in vivo (see below).

Calibration of CFMs and Enzyme-Linked Biosensors—Both the magnitude and temporal dynamics of the FPA responses to 5-second bolus applications of 2.5, 5, and 10 μ M dopamine recorded at a single CFM in the flow injection system by the WINCS were comparable to those recorded by the eDAQ system (Fig. 3A). As shown in Fig. 3B, calibration curves generated from these data for dopamine concentration versus dopamine oxidation current were linear for both systems, with a correlation coefficient of > 0.94 . In a similar fashion, linear FPA responses recorded by WINCS were also observed, with stepwise increases in beaker concentrations of glutamate and adenosine (Fig. 3C and D, respectively).

In Vivo FPA Testing of the WINCS

Dopamine Recordings—As shown in a representative animal in Fig. 4A, DBS of the MFB (60, 120, or 240 pulses at 60 Hz and 900 μ A; 4 rats) evoked a rapid increase in striatal dopamine oxidation current corresponding to stimulus time-locked increases in dopamine release.¹⁶ On cessation of each stimulation, the FPA signal returned rapidly to prestimulus levels as a result of terminal dopamine reuptake.^{42,43} Comparable FPA signals were recorded with both the WINCS and the eDAQ system. Systemic intraperitoneal administration of the selective dopamine reuptake inhibitor nomifensine (10 mg/kg; 2 rats) increased MFB stimulation-evoked dopamine oxidation current and delayed recovery to prestimulation baseline levels. A representative WINCS recording is shown in Fig. 4B. In contrast, combined systemic intraperitoneal administration of the selective serotonin (fluoxetine) and norepinephrine (desipramine) reuptake inhibitors (10 mg/kg each; 2 rats) failed to alter the magnitude or temporal pattern of the FPA signal evoked by MFB stimulation (Fig. 4C).

Further confirmation that WINCS-based FPA selectively recorded striatal dopamine release evoked by MFB stimulation is shown in Fig. 4D. In a separate rat, application of FSCV with the WINCS during MFB stimulation (1 second, 60 Hz, 2-msec pulse width) yielded a background subtracted voltammogram and a pseudocolor plot that corresponded to the unique electrochemical signature of dopamine (Fig. 4D *inset* and *lower panel*, respectively). A plot of the temporal profile of MFB-evoked dopamine release recorded at the CFM by using FSCV also corresponded closely to the evoked response recorded with FPA (Fig. 4D, *upper panel*).

Adenosine Recordings—As recorded using an adenosine biosensor coupled with WINCS-based FPA, VL thalamic DBS resulted in delayed (20–25 seconds after the beginning of stimulation) increases in hydrogen peroxide oxidation current corresponding to local increases in adenosine extracellular concentrations, peaking \sim 1 minute after cessation of the 10-second stimulation, with a return to baseline within 2.5–5 minutes (Fig. 5). To explore the relationship between current intensity and frequency of electrical stimulation and extracellular adenosine concentration, local changes in adenosine concentration in response to electrical stimulation of the VL thalamus at various current intensities (0.5–2 mA) and fixed frequency (100 Hz), and at various frequencies (50–200 Hz) and fixed intensity (1 mA) were tested. As shown in Fig. 5, adenosine extracellular concentrations increased proportionately with increasing levels of current intensity or frequency (4 stimulations at varying intensities or frequencies in 1 rat). Adenosine concentrations were allowed to return to prestimulation baseline levels between stimulations.

Glutamate Recordings—To mimic monitoring in humans during neurosurgery, an in-house constructed, MR imaging-compatible stereotactic frame for the pig was used to compare the WINCS and eDAQ-based FPA recordings of MCS-evoked local glutamate release. Cortical 100-Hz stimulation of the pig motor cortex for 10 seconds at 1 mA was delivered to the Medtronic 3389 DBS lead across contacts 0 (negative) and 3 (positive). As shown in Fig. 6 *upper*, cortical stimulation evoked comparable increases in hydrogen peroxide oxidation currents corresponding to local glutamate release, as recorded using a glutamate biosensor coupled with the WINCS and the eDAQ system. To explore the relationship between current intensity of electrical stimulation and extracellular glutamate concentration, local changes in glutamate concentration in response to electrical stimulation of the motor cortex at various current intensities (0.5–2 mA) and frequency (100 Hz) were tested with the WINCS. As shown in Fig. 6 *lower*, glutamate extracellular concentrations increased proportionately with increasing levels of current intensity. With respect to the start of stimulation and at current intensities of 0.5, 1, 1.5, and 2 mA, peak oxidation currents were attained within 20, 30, 40, and 45 seconds and returned to baseline within 90, 240, 300, and $>$ 360 seconds, respectively.

Glutamate concentrations were allowed to return to prestimulation baseline levels between stimulations.

Discussion

In a companion article,⁸ we described the development of the WINCS for intraoperative neurochemical monitoring using FSCV in combination with a CFM during functional neurosurgery. Complementary to this, in the present paper, we report that the WINCS is able to support real-time FPA to detect extracellular concentrations of dopamine, adenosine, and glutamate in mammalian brain. In FPA recording mode, the monitoring capabilities of the WINCS are greatly expanded through detection of nonelectroactive transmitters by using enzyme-linked biosensors. These results highlight the potential utility of the WINCS to determine selectively the DBS- or MCS-mediated release of a wide range of neurotransmitters in real time. *In vitro* and *in vivo* proof-of-principle tests demonstrated that the WINCS compared favorably to a commercially available hardwired system consisting of a potentiostat (EA161 Picostat) in conjunction with an analog-to-digital signal converter-recorder (e-corder) run by Chart software. Indeed, the utility of the WINCS for intraoperative use was clearly demonstrated through its performance in the electromagnetically noisy environment of a typical neurosurgery operating room, and as demonstrated by its successful use to measure glutamate during mock neurosurgery in a pig. The WINCS may thus provide a powerful new technology for intraoperative neurochemical monitoring that is well suited for use during functional neurosurgery.

Extending the Functionality of the WINCS With FPA

The real-time, *in vivo*, electrochemical monitoring techniques of FSCV and FPA have had a great impact on the study of neurotransmission in the living brain. These techniques are well suited to the laboratory and have enabled the exploration of dynamic changes in neurotransmitter signaling (release and clearance) as a result of their subsecond temporal resolution.^{6,18} Such real-time capabilities overcome one of the major drawbacks of microdialysis, in which samples are typically acquired over several minutes.⁵ As we previously established, the WINCS effectively supports FSCV at a CFM for temporally, spatially, and chemically resolved monitoring of dopamine release in the living brain.⁸ However, only electroactive neurochemicals can be monitored with FSCV. Although this includes the monoamines dopamine, norepinephrine, and serotonin and their metabolites,²⁶ other important neurotransmitters such as glutamate remain undetectable. To expand the capabilities of the WINCS to include these chemical analytes, we combined the front-end circuitry of this system to include both FSCV and FPA. With FPA, the WINCS can electrochemically monitor such nonelectroactive neurotransmitters by using enzyme-linked biosensors as the recording (working) electrode.

At a CFM surface, molecules can be oxidized and reduced when an appropriate potential is applied. Oxidized molecules relinquish one or more electrons to the recording surface, whereas reduced molecules gain electrons.⁶ Currents generated by these faradic reactions are linear with respect to the concentration of the electroactive molecule(s), and thus correspond to direct dynamic fluxes in release and reuptake.²¹ The FPA represents one of the simplest electrochemical techniques, because the potential applied to the working electrode is held constant and the current can be monitored rapidly, being collected at a rate of > 10,000 samples/second. The background current (nonfaradic current) recorded at the electrode surface is minimal, and thus allows sensitive measurements of electrochemically active molecules. When enzymes are applied to the recording electrode surface, the interaction of a nonelectroactive ligand can produce an electrochemically active reporter molecule, such as hydrogen peroxide. This allows for selective measurement of molecules that are not directly electroactive. Thus,

when a potential is applied to this type of biosensor, it is the reporter molecule that loses electrons to the recording surface. This faradic current is then directly proportional to the analyte concentration. Because many CNS neurotransmitters are not electrochemically active, FPA in combination with enzyme-linked microelectrodes (Table 1) represents a powerful tool for rapid and selective neurochemical sampling in mammalian brain (see Dale et al.¹⁵ and Hascup et al.²¹ for review).

It is important to recognize that we used a biosensor to detect adenosine release (a device that according to the manufacturer also responds to the adenosine enzymatic products inosine, hypoxanthine, and xanthine). A strategy to avoid contamination of the FPA signal from these substances involves simultaneous recordings from a sentinel (self-referencing) sensor that is made from the same materials as the adenosine sensor, but lacks the enzyme adenosine deaminase to detect the downstream enzymatic substrates. Simultaneous recordings from an adenosine and inosine sensor on a single probe array, for example, would provide a higher degree of selectivity. Similarly, the selectivity of the glutamate biosensor used in the present study would also benefit from the coapplication of a sentinel probe lacking glutamate oxidase. In the case of glutamate biosensors, sensors incorporating sentinel probes have been developed and tested *in vivo*, and similar multisite electrode designs are being considered for the detection of adenosine.^{11,20,21,23,39} Future hardware designs for the WINCS will incorporate recording inputs for several biosensors, coupled with online direct-current differential amplifiers or offline digital subtraction of the data to yield highly selective measurements of nonelectroactive neurotransmitter substances.

Feasibility of Monitoring Neurochemicals During Neurosurgery

There is a growing body of evidence indicating that one important mechanism of action of DBS is the modulation of neurotransmitter release throughout neuronal networks.²⁹ Intracellular electrode recordings^{2,31} have shown the presence of both inhibitory and excitatory postsynaptic potentials as a consequence of HFS mimicking the parameters used in clinical DBS. However, the role of specific neurotransmitters in this phenomenon and the kinetics of release are only now beginning to be elucidated. For example, using FPA with the eDAQ system, we have previously demonstrated that unilateral HFS of the subthalamic nucleus in anesthetized rats elicits local glutamate release.³² Similarly, increases in glutamate, γ -aminobutyric acid, and dopamine release in the striatum were seen in both intact and hemiparkinsonian rats in response to DBS of the subthalamic nucleus.^{9,30} Furthermore, DBS of the thalamus has been demonstrated to induce the release of adenosine triphosphate into the extracellular space, which in turn is rapidly converted to adenosine. It has been hypothesized⁴ that DBS-mediated release of adenosine may play a major role in mediating the therapeutic efficacy of DBS for tremor, given that the ventral intermediate nucleus of the thalamus is an effective therapeutic target for treatment of essential and parkinsonian tremor.^{12,24,41} Additional evidence that adenosine is a key player in DBS-induced tremor control is based on observations in a mouse model of tremor. Intrathalamic infusions of A1 receptor agonists directly reduce tremor, with an efficacy comparable to DBS.⁴

Here, we confirm that electrical stimulation evokes neurotransmitter release, including distal release of dopamine with MFB stimulation, local release of adenosine in the VL thalamus, and of glutamate in the motor cortex. In addition, we establish that such neurotransmission can be wirelessly detected using WINCS-based FPA. Together with other studies demonstrating a key role for neurotransmitters in the therapeutic mechanism of action of DBS and MCS, this lays the groundwork for the future application of neurotransmitter sensor technology as an intraoperative neurosurgical tool and feedback device. Because this technology has not yet been applied to humans, our present goal is to ensure patient safety and to establish standardized

protocols for routine, real-time monitoring of neurotransmitters during functional neurosurgical procedures.

Taking the WINCS to the Operating Room

Extracellular microelectrode recordings are routinely conducted during DBS surgery in humans.⁴⁰ However, to our knowledge, no electrochemical recordings have been performed in humans during this interventional neurosurgical procedure, leaving unanswered the important question as to which neurotransmitter systems are actually activated during human DBS and MCS. One key limitation is the lack of an FDA-approved potentiostat to support these measurements. Several key criteria must be met to develop such instrumentation, the foremost being patient safety, signal fidelity, and integration with the existing functional neurosurgical setup. The WINCS patient module—the small, wireless, sterilizable, battery-powered unit that senses neurotransmitter redox currents—has been designed in compliance with FDA-recognized consensus standards for medical electrical device safety. The WINCS is also easily attachable to the stereotactic frame, and transmits data to a remotely located base station, thus minimizing the crowding of the busy operating room. This lays important groundwork for future human trials in which the WINCS is used to monitor neurotransmission in the intraoperative setting.

Conclusions

It is becoming increasingly clear that the neurophysiological effects of DBS at the cellular level result from alterations in neurotransmission within the thalamocortical basal ganglia circuit. This in turn highlights the potential efficacy of WINCS intraoperative technology for use in humans to elucidate the role of DBS in evoking local and distal neurotransmitter release. We propose that the WINCS be used to support intraoperative neurochemical monitoring during functional neurosurgery by using both FSCV and FPA. By incorporating FPA, the chemical repertoire of WINCS-measurable neurotransmitters is expanded to include glutamate and other nonelectroactive species for which the evolving field of enzyme-linked biosensors exists. Because many neurotransmitters are not electrochemically active, FPA in combination with enzyme-linked microelectrodes represents a powerful tool for rapid and selective sampling of important intraoperative neurochemical targets. It is our hope that the WINCS will ultimately allow neurosurgeons to know with confidence that a particular implant will be therapeutically effective in their patients.

Acknowledgments

The authors acknowledge the contribution of the engineers of the Division of Engineering of Mayo Clinic (April Home, Sidney Whitlock, David Johnson, Kenneth Kressin, Bruce Winter, and Geraldine Bernard) for their invaluable efforts in the realization of the WINCS device and software.

Disclosure: This work was supported by the following organizations: National Institutes of Health (Grant No. K08 NS 52232 to Dr. Lee); Mayo Foundation (Research Early Career Development Award for Clinician Scientist to Dr. Lee); John T. and Lillian Mathews Professorship in Neuroscience award, The Grainger Foundation, the National Science Foundation (Grant Nos. DBI-0138011 and DBI-0754615 to Dr. Garris); and Austrian Academy of Sciences (DOC-fellowship to Dr. Griessenauer). The authors report no other conflict of interest concerning the materials or methods used in this study or the findings specified in this paper.

References

1. Aillon, D.; Johnson, DA.; Gabbert, S.; Naylor, E.; Wilson, GS. Near real-time measurement of glutamate concentration using biosensors in place of traditional methodologies. In: Phillips, PEM.; Sandberg, SG.; Ahn, S., et al., editors. Proceedings of the 12th International Conference on In Vivo Methods; Vancouver: University of British Columbia; 2008. Abstract

2. Anderson T, Hu B, Pittman Q, Kiss ZH. Mechanisms of deep brain stimulation: an intracellular study in rat thalamus. *J Physiol* 2004;559:301–313. [PubMed: 15218068]
3. Bath BD, Michael DJ, Trafton BJ, Joseph JD, Runnels PL, Wightman RM. Subsecond adsorption and desorption of dopamine at carbon-fiber microelectrodes. *Anal Chem* 2000;72:5994–6002. [PubMed: 11140768]
4. Bekar L, Libionka W, Tian GF, Xu Q, Torres A, Wang X, et al. Adenosine is crucial for deep brain stimulation-mediated attenuation of tremor. *Nat Med* 2008;14:75–80. [PubMed: 18157140]
5. Benveniste H. Brain microdialysis. *J Neurochem* 1989;52:1667–1679. [PubMed: 2656913]
6. Blaha CD, Phillips AG. A critical assessment of electrochemical procedures applied to the measurement of dopamine and its metabolites during drug-induced and species-typical behaviours. *Behav Pharmacol* 1996;7:675–708. [PubMed: 11224465]
7. Bledsoe, JM.; Goerss, SJ.; Kall, B.; Gustine, B.; Forsman, R.; Felmlee, J., et al. Neuroscience 2008 Meeting Planner. Washington DC: Society for Neuroscience; 2008. MRI compatible stereotaxic head-frame and navigation software for research in pigs. 659.8/UU92 (Abstract)
8. Bledsoe JM, Kimble CJ, Covey DP, Blaha CD, Agnesi F, Mohseni P, et al. Development of the Wireless Instantaneous Neurotransmitter Concentration System for intraoperative neurochemical monitoring using fast-scan cyclic voltammetry. Technical note. *J Neurosurg*. May 8;2009 Published online. 10.3171/2009.3.JNS081348
9. Bruet N, Windels F, Carcenac C, Feuerstein C, Bertrand A, Poupard A, et al. Neurochemical mechanisms induced by high frequency stimulation of the subthalamic nucleus: increase of extracellular striatal glutamate and GABA in normal and hemiparkinsonian rats. *J Neuropathol Exp Neurol* 2003;62:1228–1240. [PubMed: 14692699]
10. Burmeister, JJ.; Pomerleau, F.; Huettl, P.; Gerhardt, GA. Advances in the in vivo detection of GABA using enzyme coated microelectrode arrays. In: Phillips, PEM.; Sandberg, SG.; Ahn, S., et al., editors. Proceedings of the 12th International Conference on In Vivo Methods; Vancouver: University of British Columbia; 2008. Abstract
11. Burmeister JJ, Pomerleau F, Palmer M, Day BK, Huettl P, Gerhardt GA. Improved ceramic-based multisite microelectrode for rapid measurements of L-glutamate in the CNS. *J Neurosci Methods* 2002;119:163–171. [PubMed: 12323420]
12. Busenbark K, Barnes P, Lyons K, Ince D, Villagra F, Koller WC. Accuracy of reported family histories of essential tremor. *Neurology* 1996;47:264–265. [PubMed: 8710092]
13. Cechova S, Venton BJ. Transient adenosine efflux in the rat caudate-putamen. *J Neurochem* 2008;105:1253–1263. [PubMed: 18194431]
14. Dale N, Gourine AV, Llaudet E, Bulmer D, Thomas T, Spyer KM. Rapid adenosine release in the nucleus tractus solitarii during defense response in rats: real-time measurement in vivo. *J Physiol* 2002;544:149–160. [PubMed: 12356888]
15. Dale N, Hatz S, Tian F, Llaudet E. Listening to the brain: microelectrode biosensors for neurochemicals. *Trends Biotechnol* 2005;23:420–428. [PubMed: 15950302]
16. Dugast C, Suaud-Chagny MF, Gonon F. Continuous in vivo monitoring of evoked dopamine release in the rat nucleus accumbens by amperometry. *Neuroscience* 1994;62:647–654. [PubMed: 7870296]
17. Garguilo MG, Michael AC. Amperometric microsensors for monitoring choline in the extracellular fluid of brain. *J Neurosci Methods* 1996;70:73–82. [PubMed: 8982984]
18. Garris, PA.; Greco, PG.; Sandberg, SG.; Howes, G.; Pongmaytegul, S.; Heidenreich, BA., et al. In vivo voltammetry with telemetry. In: Michael, AC.; Borland, LM., editors. *Electrochemical Methods for Neuroscience*. Boca Raton, FL: CRC Press; 2006. p. 233-260.
19. Gourine AV, Llaudet E, Thomas T, Dale N, Spyer KM. Adenosine release in nucleus tractus solitarii does not appear to mediate hypoxia-induced respiratory depression in rats. *J Physiol* 2002;544:161–170. [PubMed: 12356889]
20. Hascup, ER.; Hascup, KN.; Hinzman, JM.; Pomerleau, F.; Huettl, P.; Johnson, KW., et al. Determining the source of resting and physiologically-evoked L-glutamate levels using enzyme-based microelectrode arrays in awake rats. In: Phillips, PEM.; Sandberg, SG.; Ahn, S., et al., editors. Proceedings of the 12th International Conference on In Vivo Methods; Vancouver: University of British Columbia; 2008. Abstract

21. Hascup, KN.; Rutherford, EC.; Quintero, JE.; Day, BK.; Nickell, JR.; Pomerleau, F., et al. Second-by-second measures of L-glutamate and other neurotransmitters using enzyme-based microelectrode arrays. In: Michael, AC.; Borland, LM., editors. *Electrochemical Methods for Neuroscience*. Boca Raton, FL: CRC Press; 2006. p. 407-450.
22. Henderson JM, Lad SP. Motor cortex stimulation and neuropathic facial pain. *Neurosurg Focus* 2006;26(6):E6. [PubMed: 17341050]
23. Hinzman, JM.; Lisembee, A.; Huettl, P.; Pomerleau, F.; Lifshitz, J.; Gerhardt, GA. Alterations in glutamate neurotransmission after traumatic brain injury: study using enzyme-based microelectrode arrays. In: Phillips, PEM.; Sandberg, SG.; Ahn, S., et al., editors. *Proceedings of the 12th International Conference on In Vivo Methods*; Vancouver: University of British Columbia; 2008. Abstract
24. Hubble JP, Busenbark KL, Wilkinson S, Penn RD, Lyons K, Koller WC. Deep brain stimulation for essential tremor. *Neurology* 1996;46:1150-1153. [PubMed: 8780109]
25. Huffman ML, Venton BJ. Carbon-fiber microelectrodes for in vivo applications. *Analyst* 2009;134:18-24. [PubMed: 19082168]
26. Justice, JB, Jr. *Voltammetry in the Neurosciences: Principles, Methods, and Applications*. Clifton NJ: Humana Press; 1987.
27. Konradsson, A.; Gash, CR.; Gerhardt, GA.; Bruno, JP. Second-by-second measurement of stimulated glutamate release and its modulation by $\alpha 7$ and mGlu 2/3 receptors: relevance to schizophrenia. In: Phillips, PEM.; Sandberg, SG.; Ahn, S., et al., editors. *Proceedings of the 12th International Conference on In Vivo Methods*; Vancouver: University of British Columbia; 2008. Abstract
28. Kristensen EW, Wilson RL, Wightman RM. Dispersion in flow injection analysis measured with microvoltammetric electrodes. *Anal Chem* 1986;58:986-988.
29. Lee KH, Blaha CD, Garris PA, Mohseni P, Horne AE, Bennet KE, et al. Evolution of deep brain stimulation: human electrometer and smart devices supporting the next generation of therapy. *Neuromodulation* 2009;12 in press.
30. Lee KH, Blaha CD, Harris BT, Cooper S, Hitti FL, Leiter JC, et al. Dopamine efflux in the rat striatum evoked by electrical stimulation of the subthalamic nucleus: potential mechanism of action in Parkinson's disease. *Eur J Neurosci* 2006;23:1005-1014. [PubMed: 16519665]
31. Lee KH, Chang SY, Roberts DW, Kim U. Neurotransmitter release from high-frequency stimulation of the subthalamic nucleus. *J Neurosurg* 2004;101:511-517. [PubMed: 15352610]
32. Lee KH, Kristic K, van Hoff R, Hitti FL, Blaha CD, Harris B, et al. High-frequency stimulation of the subthalamic nucleus increases glutamate in the subthalamic nucleus of rats as demonstrated by in vivo enzyme-linked glutamate sensor. *Brain Res* 2007;1162:121-129. [PubMed: 17618941]
33. Llaudet E, Botting NP, Crayston JA, Dale N. A three-enzyme microelectrode sensor for detecting purine release from central nervous system. *Biosens Bioelectron* 2003;18:43-52. [PubMed: 12445443]
34. Lowry JP, Fillenz M. Real-time monitoring of brain energy metabolism in vivo using microelectrochemical sensors: the effects of anesthesia. *Bioelectrochemistry* 2001;54:39-47. [PubMed: 11506973]
35. Lowry JP, Miele M, O'Neill RD, Boutelle MG, Fillenz M. An amperometric glucose-oxidase/poly (o-phenylenediamine) biosensor for monitoring brain extracellular glucose: in vivo characterization in the striatum of freely-moving rats. *J Neurosci Methods* 1998;79:65-74. [PubMed: 9531461]
36. Mitchell KM. Acetylcholine and choline amperometric enzyme sensors characterized in vitro and in vivo. *Anal Chem* 2004;76:1098-1106. [PubMed: 14961744]
37. Naylor, E.; Aillon, D.; Harmon, H.; Gabbert, S.; Johnson, D.; Johnson, DA., et al. A new technique for the simultaneous recording of electroencephalograph activity and CNS biosensor data. In: Phillips, PEM.; Sandberg, SG.; Ahn, S., et al., editors. *Proceedings of the 12th International Conference on In Vivo Methods*; Vancouver: University of British Columbia; 2008. Abstract
38. Netchiporouk L, Shram N, Salvert D, Cespuglio R. Brain extracellular glucose assessed by voltammetry throughout the rat sleep-wake cycle. *Eur J Neurosci* 2001;13:1429-1434. [PubMed: 11298804]
39. Pomerleau F, Day BK, Huettl P, Burmeister JJ, Gerhardt GA. Real time in vivo measures of L-glutamate in the rat central nervous system using ceramic-based multisite microelectrode arrays. *Ann N Y Acad Sci* 2003;1003:454-457. [PubMed: 14684487]

40. Priori A, Egesi M, Pesenti A, Rohr M, Rampini P, Locatelli M, et al. Do intraoperative microrecordings improve subthalamic nucleus targeting in stereotactic neurosurgery for Parkinson's disease? *J Neurosurg Sci* 2003;47:56–60. [PubMed: 12900734]
41. Rehnroona S, Johnels B, Widner H, Törnqvist AL, Hariz M, Sydow O. Long-term efficacy of thalamic deep brain stimulation for tremor: double-blind assessments. *Mov Disord* 2003;18:163–170. [PubMed: 12539209]
42. Suaud-Chagny MF. In vivo monitoring of dopamine overflow in the central nervous system by amperometric techniques combined with carbon fibre electrodes. *Methods* 2004;33:322–329. [PubMed: 15183181]
43. Suaud-Chagny MF, Dugast C, Chergui K, Mghina M, Gonon F. Uptake of dopamine released by impulse flow in the rat mesolimbic and striatal systems in vivo. *J Neurochem* 1995;65:2603–2611. [PubMed: 7595557]
44. Thomas L, Bledsoe JM, Stead S, Sandroni P, Gorman D, Lee KH. Motor cortex and deep brain stimulation for the treatment of intractable neuropathic face pain. *Curr Neurol Neurosci Rep* 2009;9:120–126. [PubMed: 19268035]
45. Tsubokawa T, Katayama Y, Yamamoto T, Hirayama T, Koyama S. Chronic motor cortex stimulation in patients with thalamic pain. *J Neurosurg* 1993;78:393–401. [PubMed: 8433140]

Abbreviations used in this paper

AP	anteroposterior
CFM	carbon-fiber microelectrode
DBS	deep brain stimulation
DV	dorsoventral
FPA	fixed potential amperometry
FSCV	fast-scan cyclic voltammetry
HFS	high-frequency stimulation
MCS	motor cortex stimulation
MFB	medial forebrain bundle
ML	mediolateral
PBS	phosphate-buffered saline
VL	ventrolateral
WINCS	Wireless Instantaneous Neurotransmitter Concentration System

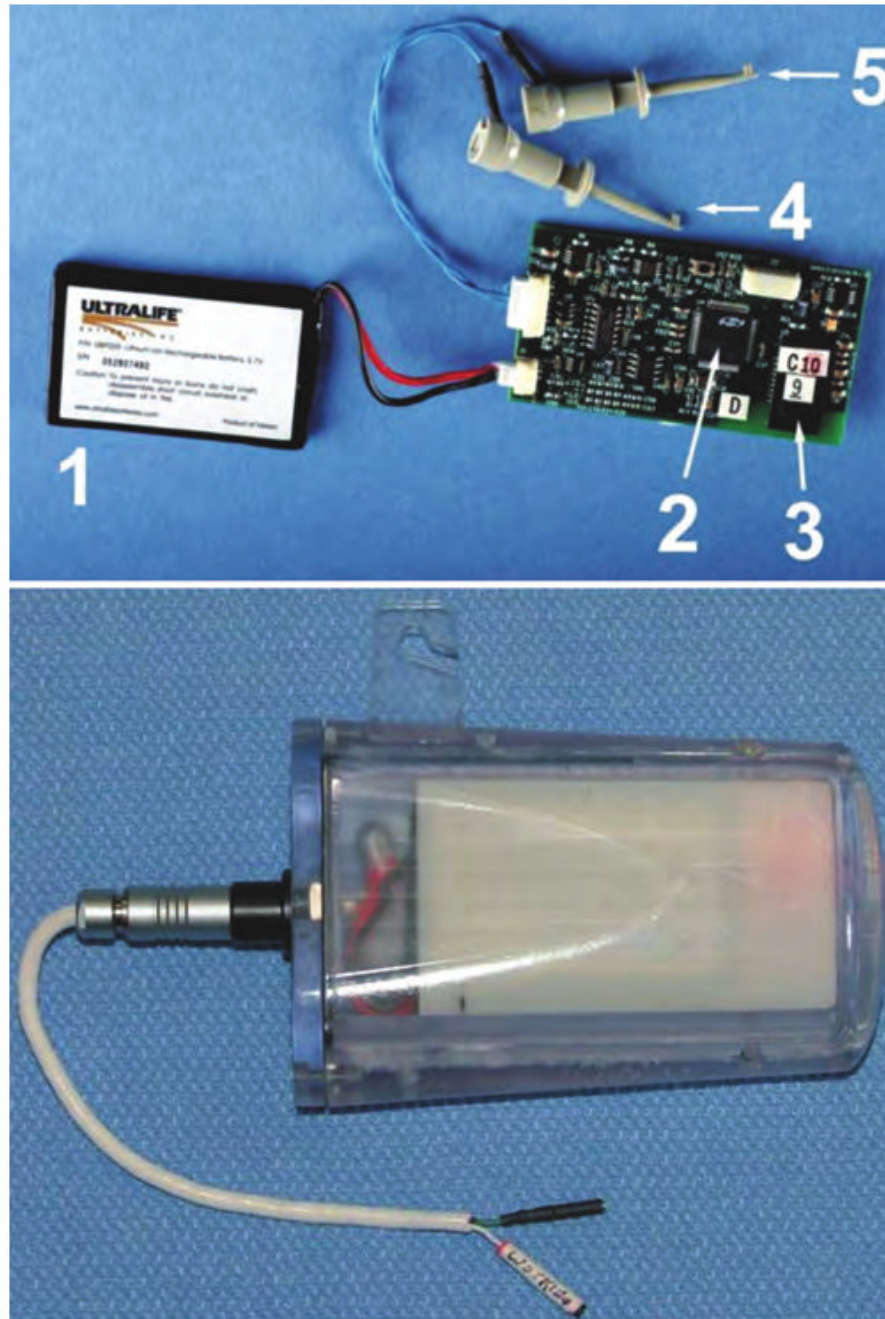


Fig. 1.
Upper: Photograph showing the battery (1); microprocessor (2); Bluetooth chip (3); working electrode lead (4); and reference/counter electrode lead (5) of the monitoring device. *Lower:* Photograph showing the WINCS device encased in its sterilizable polycarbonate case.

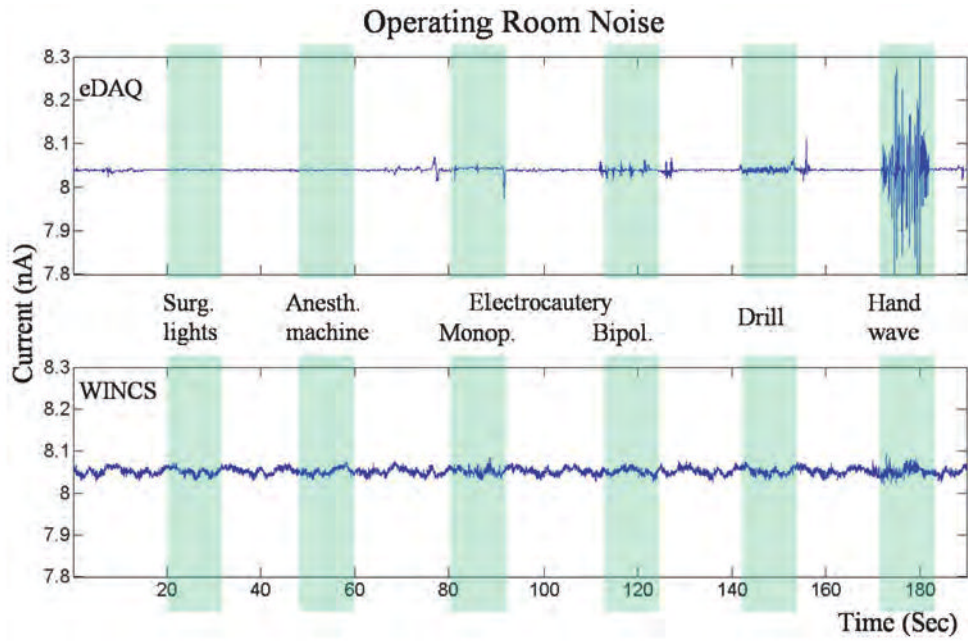


Fig. 2. Tracings showing a comparison of the WINCS with the eDAQ system for susceptibility to noise in the operating room environment during FPA. A 100-M Ω dummy cell was connected to each system, and they were placed on the operating room table within 1 foot of each other. Hand waving and electrical devices (surgical lights, anesthesia machine, electrocauterizer, and pneumatic hand drill), turned on (*blue bar*) and off at various intervals, were applied 1 foot above the dummy cell. Anesth. = anesthesia; bipol. = bipolar; monop. = monopolar; Surg. = surgical.

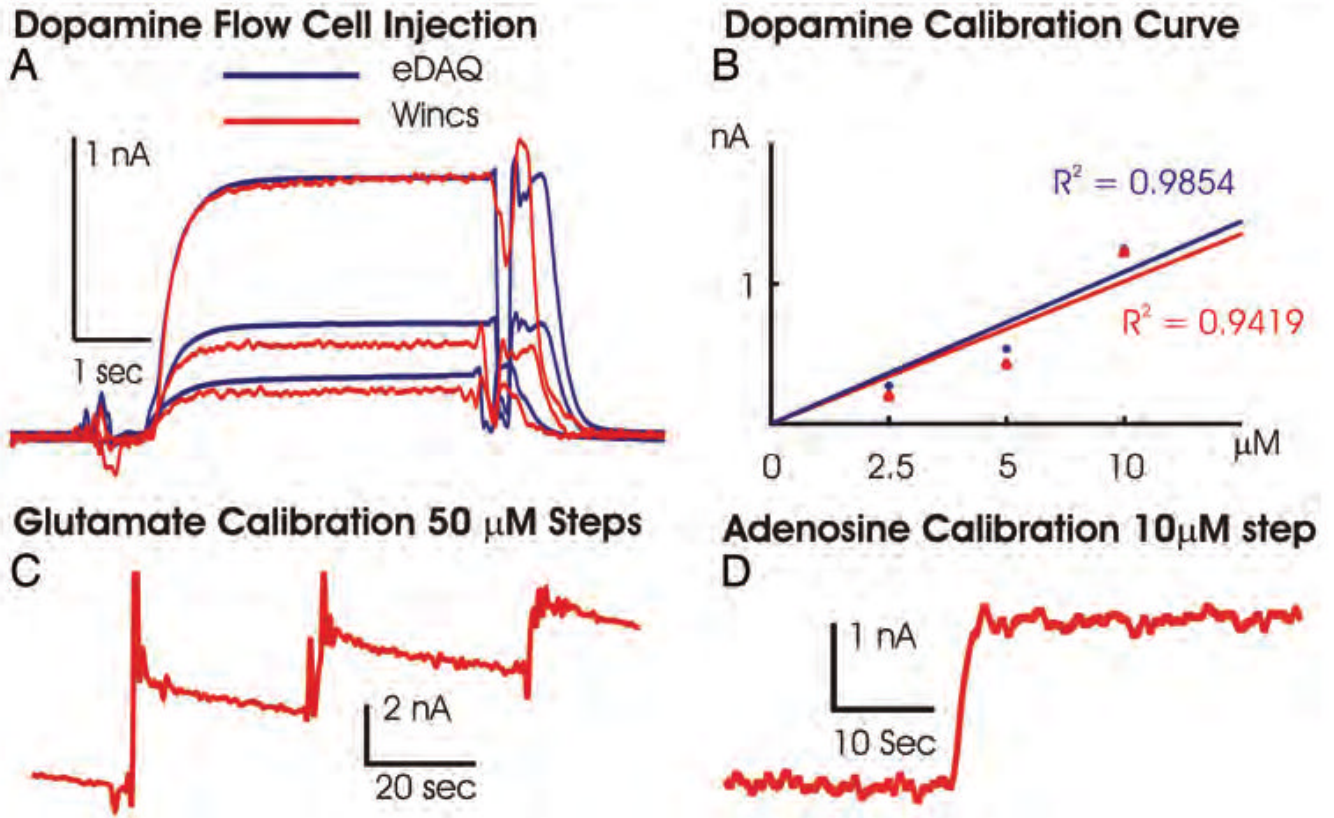


Fig. 3.
 A: Chart showing data obtained after 5-second-long bolus injections of 2.5, 5, and 10 μM dopamine across a single CFM in the flow cell, measured with the WINCS (red line) and a hardwired potentiostat system (eDAQ, blue line). B: Plot of dopamine oxidation current versus dopamine concentrations and linear regression analysis for both FPA recordings made using the WINCS and the eDAQ system. The perturbations in the amperometric signals occurring at the start and end of the 5-second bolus injections of dopamine are a result of engaging and disengaging the electronic valve and do not interfere with the calibration assessments. C: The WINCS glutamate sensor calibration, oxidation current for three 50- μM glutamate concentration steps. D: Calibration of adenosine biosensor performed with a single 10- μM concentration step, as measured with the WINCS.

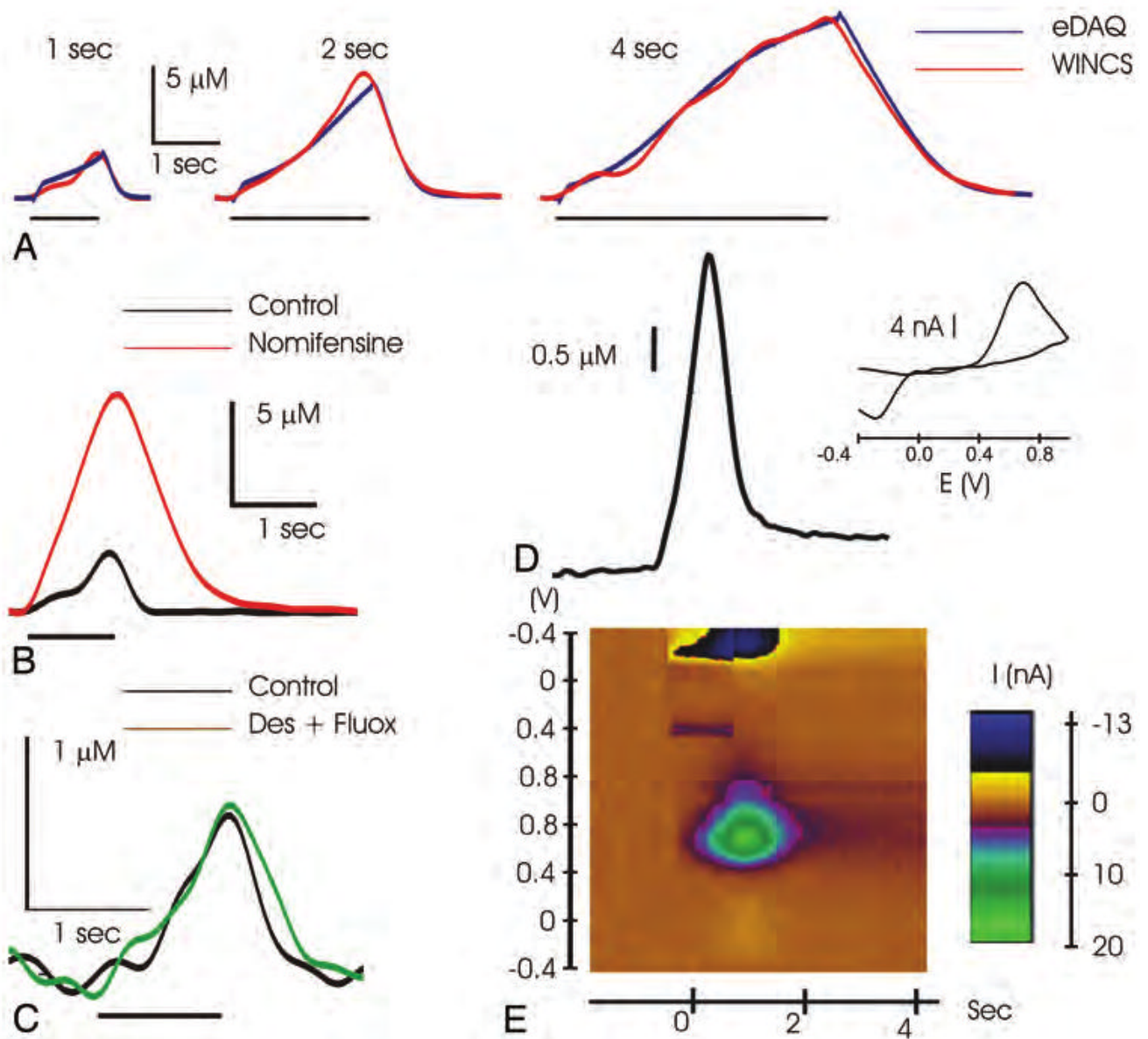


Fig. 4.
 A: Graph showing striatal dopamine release evoked by 1, 2, or 4 seconds of 60-Hz MFB stimulation (*black bars*), as measured with the WINCS (*red lines*) and a hardwired system (eDAQ, *blue lines*). B: Graph showing that systemic administration of the dopamine reuptake inhibitor nomifensine induced an increase and delay in recovery of the evoked signal, confirming the dopaminergic origin of the measured current. C: Graph showing that systemic administration of the norepinephrine and serotonin reuptake inhibitors desipramine (Des) and fluoxetine (Fluox), respectively, failed to increase the amperometric signal, indicating a lack of interference from these 2 neurotransmitters in the striatum. Graph (D) and pseudocolor plot (E) showing striatal dopamine release as measured with the WINCS in FSCV mode during 1-second MFB stimulation. The oxidation and reduction peak potential as shown in the voltammogram (*inset*) and pseudocolor plot further indicates that the FSCV signal corresponds to dopamine oxidation (*green spot*) and reduction (*dark spot*) current.

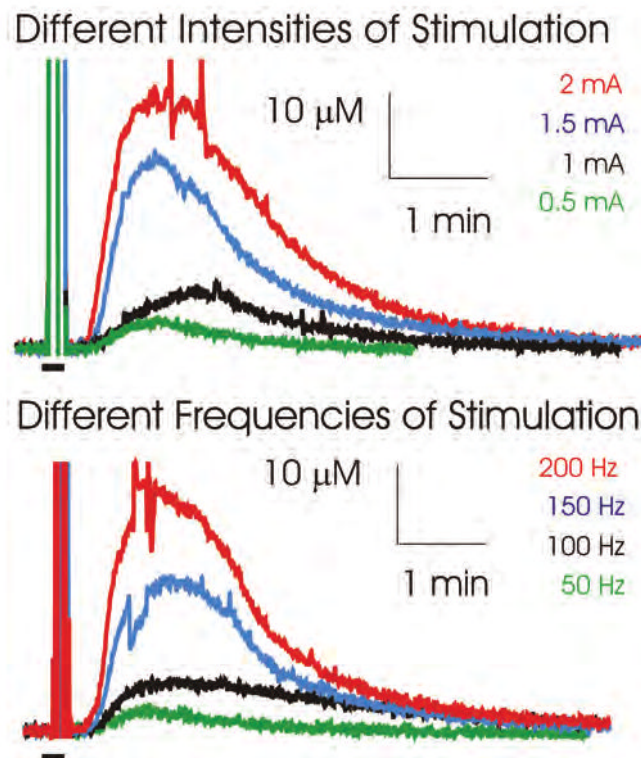
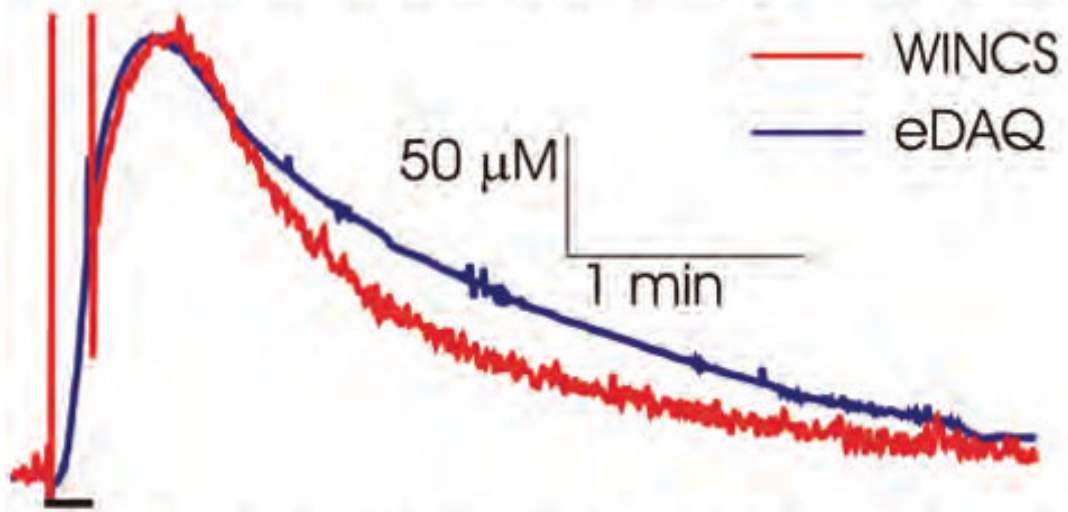


Fig. 5. *Upper:* Graph showing that VL thalamic stimulation (100 Hz, 10-second duration) at different intensities (0.5–2 mA) evoked progressively larger increases in local extracellular concentrations of adenosine. *Lower:* Graph showing that increasing VL thalamic stimulation frequency from 50 to 100 Hz at 1 mA also evoked progressively larger increases in local extracellular concentrations of adenosine. *Black bars* on the lower left side in each panel represent the duration of stimulation, and *vertical lines* above these bars are recording artifacts that occurred during stimulation.

Glutamate release during 1 mA HFS



HFS Induced Glutamate Release

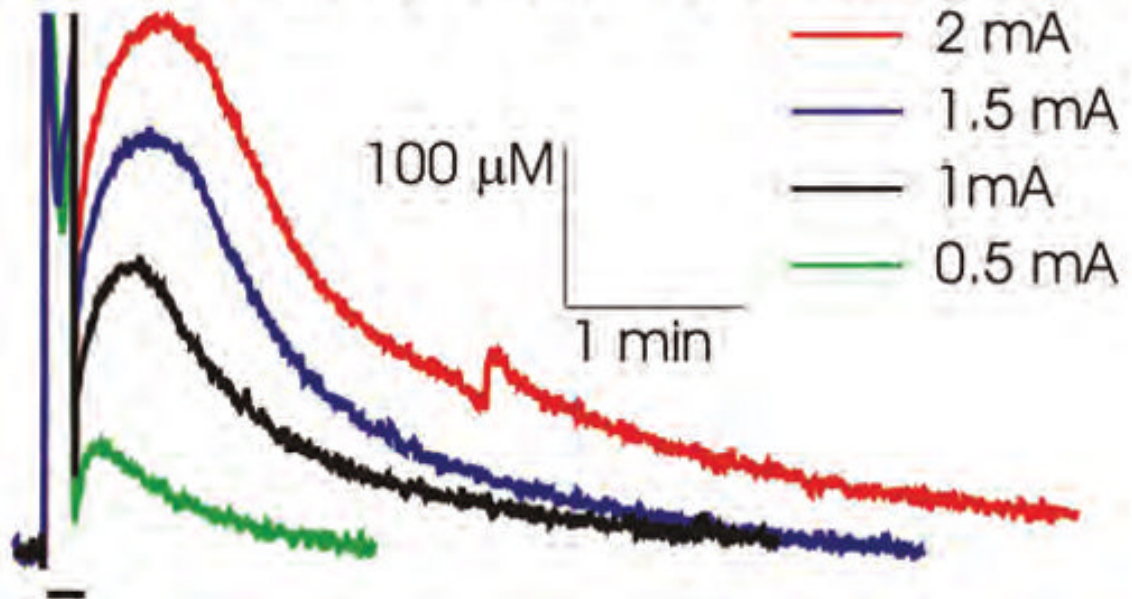


Fig. 6.

Upper: Graph showing that cortical stimulation (100 Hz at 1 mA for 10 seconds) in the pig increased local extracellular concentrations of glutamate measured with the WINCS (*red line*) and with a hardwired system (eDAQ, *blue line*). *Lower:* Graph showing that increasing the cortical stimulation intensity from 0.5 to 2 mA at 100 Hz evoked progressively larger increases in local extracellular concentrations of glutamate. *Black bars* on the lower left side in each panel represent the duration of stimulation, and *vertical lines* above these bars are recording artifacts that occurred during stimulation.

TABLE 1
Literature review of FPA-compatible enzyme-linked microelectrodes for selective real-time monitoring of neurochemicals in mammalian brain *

Analyte	Preclinical Applications	Molecule
glutamate	HFS-evoked glutamate release & clearance in vivo ³⁰	E: glutamate oxidase
	glutamate transmission after TBI ²⁰	R: hydrogen peroxide
	KCl-induced glutamate release in vivo & in vitro ^{11,39}	
	ketamine-induced glutamate release in freely moving rats ¹	
	prefrontal glutamate release evoked by PCP local infusions ²⁷	
GABA	alterations in glutamate neurotransmission after TBI ²³	E ₁ : γ -aminobutyric glutamate transaminase
		E ₂ : succinic semialdehyde dehydrogenase
adenosine	detection of exogenous GABA in vivo ¹⁰	E ₃ : glutamate oxidase
	release from spinal cord during locomotion in vivo ³³	R: hydrogen peroxide
	release from brainstem during cardiorespiratory & defense reflexes in vivo ^{14,19}	E ₁ : adenosine deaminase
acetylcholine/choline	detection of exogenous choline & endogenous cholinesterase activity in vivo ^{17,36}	E ₂ : nucleoside phosphorylase
		E ₃ : xanthine oxidase
		R: hydrogen peroxide
glucose	effect of anesthesia on glucose levels in vivo ³⁴	E ₁ : acetylcholine esterase
	glucose levels in striatum in freely moving rats ³⁵ & in cortex during sleep/wake cycle ³⁸	E ₂ : choline oxidase
	correlations of EEG/EMG activity with fluctuations in cortical glucose levels ³⁷	R: hydrogen peroxide

* E = enzyme; EEG = electroencephalography; EMG = electromyography; GABA = γ -aminobutyric acid; PCP = phencyclidine; R = reporter; TBI = traumatic brain injury.